ELSEVIER

FEMS Microbiology Letters 204 (2001) 247–252

FEMS MICROBIOLOGY Letters

www.fems-microbiology.org

Metabolic flux response to phosphoglucose isomerase knock-out in *Escherichia coli* and impact of overexpression of the soluble transhydrogenase UdhA

Fabrizio Canonaco [a], Tracy A. Hess [b], Sylvia Heri [a], Taotao Wang [b], Thomas Szyperski [b], Uwe Sauer [a,*]

[a] *Institute of Biotechnology, ETH Zürich, CH-8093 Zurich, Switzerland*

[b] *Department of Chemistry, University at Buffalo, The State University of New York, Buffalo, NY 14260, USA*

Received 16 May 2001; received in revised form 22 August 2001; accepted 23 August 2001

First published online 5 October 2001

Abstract

Blocking glycolytic breakdown of glucose by inactivation of phosphoglucose isomerase (Pgi) in *Escherichia coli* led to a greatly reduced maximum specific growth rate. Examination of the operational catabolic pathways and their flux ratios using [*U*-$^{13}C_6$]glucose-labeling experiments and metabolic flux ratio analysis provide evidence for the pentose phosphate (PP) pathway as the primary route of glucose catabolism in the knock-out mutant. The resulting extensive flux through the PP pathway disturbs apparently the reducing power balance, since overexpression of the recently identified soluble transhydrogenase UdhA improves significantly the growth rate of the Pgi mutant. The presented results provide first evidence that UdhA restores the cellular redox balance by catalyzing electron transfer from NADPH to NADH.

Keywords: Fluxome; Metabolism; Metabolic flux ratio analysis; NADPH; Phosphoglucose isomerase; Transhydrogenase

1. Introduction

By providing energy, building blocks, and co-factors, central carbon metabolism constitutes the biochemical backbone of all cells. Nevertheless, our understanding of systemic properties of the central metabolic network lacks behind the accumulated wealth of detailed biochemical and genetic knowledge on its individual components. One reason is the redundancy of this complex network, in the sense that more than one reaction or pathway catalyze a given conversion of intermediates. Thus, firm conclusions on metabolic consequences of genetic manipulations can often not be drawn on the basis of physiological characterization only [1]. When based on isotopic tracer data, however, methods of metabolic flux analysis can potentially distinguish between alternative pathways [2–4].

One approach is based on tracing intact carbon fragments in cells grown on mixtures of uniformly [*U*-$^{13}C_6$] and unlabeled glucose [5,6]. The resulting ^{13}C-labeling patterns of metabolic intermediates are analyzed by nuclear magnetic resonance (NMR) spectroscopy of amino acids that are synthesized from these intermediates. Because alternative pathways that lead to common intermediates or products yield different intact fragments that originate from a single glucose source molecule, specific multiplet patterns in the ^{13}C fine structures that reflect the in vivo usage of reactions are generated. Probabilistic equations relate the determined intensities of the multiplet components to the relative abundance of intact carbon fragments [5]. Thus, this method, also referred to as metabolic flux ratio (METAFoR) analysis, identifies the active metabolic pathways and the ratios of their fluxes during a labeling experiment [5–9].

Here we use METAFoR analysis by NMR to investigate the metabolic consequences of phosphoglucose isomerase (Pgi) inactivation in *Escherichia coli*. Since Pgi is located at the first juncture of different pathways for glucose catabolism (Fig. 1), its inactivation is particularly useful for studying general metabolic network behavior because glucose catabolism must then proceed via the pentose phosphate (PP) and/or the Entner–Doudoroff (ED)

* Corresponding author. Tel.: +41 (1) 633 36 72; Fax: +41 (1) 633 10 51.

E-mail address: sauer@biotech.biol.ethz.ch (U. Sauer).

0378-1097/01/$20.00
PII: S0378-1097(01)00407-4

pathway. This flux rerouting has a profound influence on the balance of the reducing power budget because NADPH is formed in large excess when catabolism proceeds exclusively via these pathways. In contrast to NADH, NADPH is solely used in anabolic reactions and not in respiration [10]. If and to which extend the energy-coupled, membrane-bound transhydrogenase PntAB and/or the soluble transhydrogenases UdhA are involved in maintaining the balance between NADH and NADPH in *E. coli* is currently an exciting matter of debate.

2. Materials and methods

2.1. Strains and growth conditions

Here we used the two *E. coli* strains wild-type MG1655 (λ^-, F^-, *rph-1*) and a Pgi mutant (λ^-, F^-, IN(*rrnD–rrnE*)1, *rph-1*, *pgi*::Tn10) (a gift of G. Sprenger, Biotechnology, Forschungszentrum Julich, Germany) that was constructed by P1 phage transduction of the *pgi*–Tn10 marker [11] into W3110. Luria–Bertani (LB) and M9 minimal medium were prepared as described previously [9]. M9 medium was supplemented with either glucose or fructose at a final concentration of 0.5% (w/v). Aerobic cultivation was performed in 1-l baffled shake flasks with maximally 150 ml medium at 30°C on a gyratory shaker at 200 rpm.

For ^{13}C-labeling experiments, cultures were grown in M9 medium with 0.45% (w/v) unlabeled glucose and 0.05% (w/v) uniformly labeled [*U*-$^{13}C_6$]glucose ($^{13}C > 98\%$, Isotech). In these cases, the inoculum volume was well below 1% of the culture volume, so that the presence of unlabeled biomass could be neglected for the analysis of the ^{13}C-labeling patterns. These cultures were always harvested in the mid-exponential growth phase at an optical density at 600 nm (OD_{600}) of about 1.

2.2. Analytical procedures

Cell growth was monitored by determination of OD_{600} and cellular dry weight (cdw) was calculated from previously determined OD_{600}-to-cdw correlations. Glucose, acetate, and protein concentrations were determined with commercial kits (Beckman) or by high-performance liquid chromatography (HPLC). Physiological parameters were calculated as described previously [9].

To prepare crude cell extracts, LB-grown cultures were washed and resuspended in one volume 0.9% (w/v) NaCl, 10 mM $MgSO_4$, and disrupted by two sonication steps at 100 W for 1 min each. After centrifugation at $10\,000 \times g$ for 30 min, the supernatant was transferred to a new tube and used directly for determination of protein concentration and enzyme activities. Specific activities of Pgi [12] and transhydrogenase [13,14] were determined as described previously. Specific ED-pathway activity was determined from the combined Edd and Eda reactions in a 750-μl mixture containing 5 mM 6PG, 10 mM $MgSO_4$, and 200 mM Tris–HCl (pH 7.2). The reaction was started by adding 50 μl crude cell extract and was incubated at 30°C for 30 min. After addition of 750 μl 0.2% (w/v) 2,4-dinitrophenylhydrazine in 500 mM HCl, incubation at room temperature for 10 min, and stopping the reaction by adding 500 μl 4 M NaOH, the reaction product, pyruvate, was detected by recording the extinction at 450 nm [15].

2.3. NMR spectroscopy and data analysis

Preparation of protein hydrolysates and recording of 2D ^{13}C–^{1}H correlation NMR spectra for aliphatic and aromatic amino acid resonances were performed as described previously [5,9]. The program FCAL [6,16] was used for integration of ^{13}C–^{13}C scalar coupling fine structures and the calculation of relative abundances, *f*, of intact carbon fragments originating from a single source molecule of glucose [5]. Briefly, these *f* values were calculated with probabilistic equations from the relative intensities, *I*, of the superimposed multiplets in the ^{13}C–^{13}C scalar coupling fine structures of resonances in 48 carbon atoms of the amino acids. The *f* values in amino acids carbon atoms provide then information on the metabolic origin of their precursors molecules in central metabolism, i.e. P5P, E4P, PGA, PEP, PYR, OGA, and OAA [5].

2.4. Genetic manipulations

Inducible overexpression of the soluble transhydrogenase UdhA [17] was achieved by PCR amplification of *udhA* from chromosomal DNA of *E. coli* MG1655 with the primers 5′-CGGGATCCGA TGCCATAGTA ATAGG-3′ and 5′-CCCAAGCTTT TTTAAAACAG GCGGTT-3′ (chromosomal sequences are underlined). The resulting PCR product was digested with *Bam*HI and *Hin*dIII and cloned under the control of the IPTG-inducible *trc* promoter of p*Trc99*A (Pharmacia).

3. Results and discussion

3.1. Phenotypic characterization

Pgi enzyme activities of 966 ± 5 and 5 ± 5 U mg^{-1} protein in crude cell extracts from control and mutant batch cultures, respectively, proved complete absence of Pgi activity in the mutant. Under aerobic conditions, mutant cultures grew well on fructose as the sole carbon source with a maximum specific growth rate (μ_{max}) of 0.40 h^{-1}, as was reported previously [12]. This indicates that G6P is not an essential component of *E. coli* biomass because it cannot be synthesized from fructose in *pgi*$^-$ mutants. Pro-

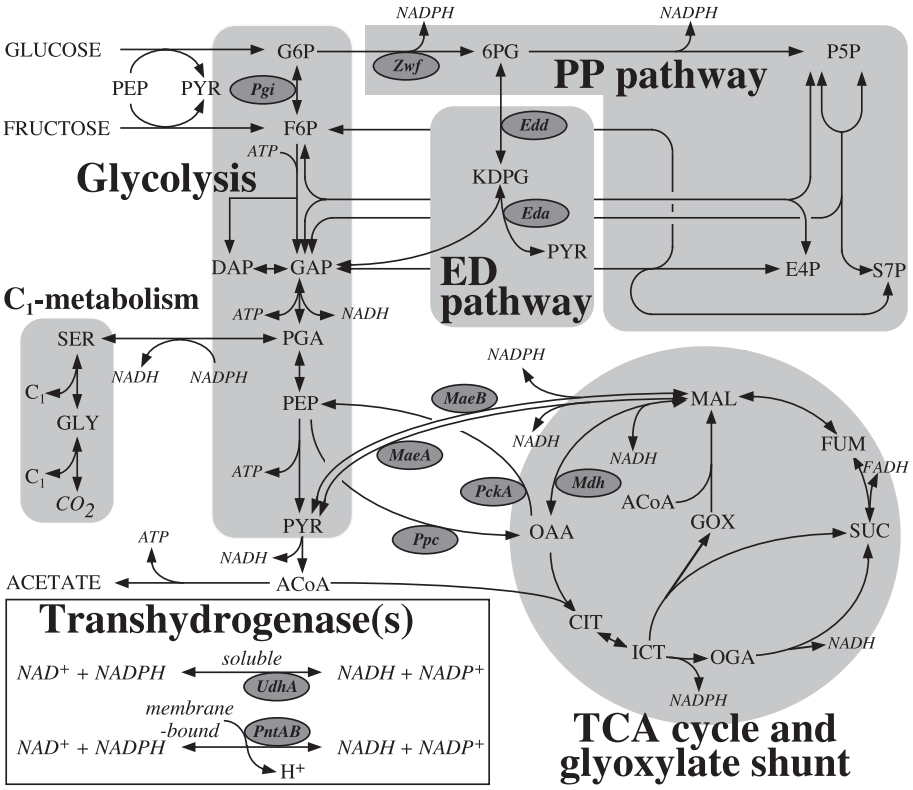

Fig. 1. Reaction network of *E. coli* central carbon metabolism. The arrows indicate physiological reaction directionality and key enzymes are indicated by their three-letter code in the gray ellipses. Abbreviations: G6P, glucose-6-phosphate; F6P, fructose-6-phosphate; 6PG, 6-phosphogluconate; KDPG, 2-keto-3-deoxy 6PG; P5P, pentose-5-phosphate; E4P, erythrose-4-phosphate; S7P, seduheptulose-7-phosphate; GAP, glyceraldehyde-3-phosphate; DAP, dihydroxy acetone-phosphate; PGA, 3-phosphoglycerate; SER, serine; GLY, glycine; PEP, phosphoenolpyruvate; PYR, pyruvate; ACoA, acetyl coenzyme A; CIT, citrate; ICT, isocitrate; OGA, oxoglutarate; SUC, succinate; FUM, fumarate; MAL, malate; OAA, oxaloacetate; GOX, glyoxylate; Eda, KDPG aldolase; Edd, 6-phosphogluconate dehydratase; Ppc, PEP carboxylase; PckA, PEP carboxykinase; Mdh, malate dehydrogenase; MaeA, NAD-linked malic enzyme; MaeB, NADP-linked malic enzyme; transhydrogenase, pyridine nucleotide transhydrogenase; Zwf, G6P dehydrogenase.

viding glucose as the sole carbon source, the Pgi mutant grew significantly slower and consumed less glucose (Table 1). The biomass yield of the Pgi mutant on glucose, however, was slightly improved when compared with the wild-type, which is consistent with previous observations [12]. This indicates a kinetic limitation of glucose catabolism, which is supported by the complete absence of the metabolic overflow product, acetate (data not shown).

3.2. Metabolic flux response to pgi knock-out

To investigate metabolic consequences of blocking the first step of glycolysis, *E. coli* wild-type and the Pgi mutant were subjected to a [*U*-$^{13}C_6$]glucose-labeling experiment in batch culture. Visual inspection of the resulting ^{13}C–^{13}C scalar coupling fine structures in the amino acids immediately revealed several striking differences between wild-type and mutant (Fig. 2). Using probabilistic equations (METAFoR analysis), these fine structures were then quantitatively analyzed and then recruited to derive METAFoRs [5,6].

The ratios obtained for MG1655 (Fig. 3) were very similar to those reported for *E. coli* JM101 when grown under the identical conditions [9]. In accordance with textbook knowledge [10], the glyoxylate shunt (Fig. 3H) and the gluconeogenic reactions catalyzed by PckA and MaeA/B (Fig. 3F,G) were inactive during aerobic exponential growth on glucose. The only significant difference between MG1655 and JM101 was the relative flux through the anaplerotic Ppc reaction, 72% (Fig. 3E) and 45% [9], respectively. The comparably high value of MG1655 demonstrates that it uses the trichloroacetic acid (TCA) cycle predominantly for generating the building blocks OAA and OGA, and to a lesser extent for generating ATP via oxidative phosphorylation. *E. coli* JM101, on the other

Table 1
Exponential growth parameters of aerobic *E. coli* cultures with glucose as the sole carbon source

Parameter	Wild-type	Pgi mutant
μ_{max} (h^{-1})	0.74 ± 0.02[a]	0.16 ± 0.01
q_{glc} (g g^{-1} h^{-1})[b]	2.4 ± 0.1	1.1 ± 0.1
$Y_{X/S}$ (g g^{-1})[c]	0.46 ± 0.03	0.54 ± 0.02

[a]Standard deviation from triplicate experiments.
[b]Specific glucose consumption rate.
[c]Yield of biomass on glucose during the exponential growth phase.

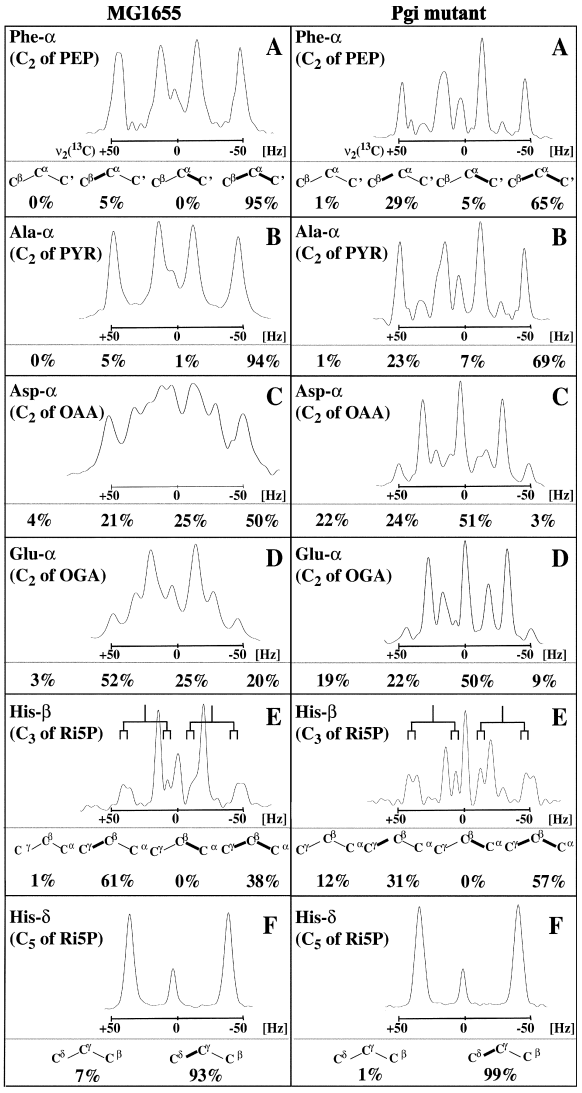

Fig. 2. ^{13}C scalar coupling fine structures observed for fractionally ^{13}C-labeled amino acids obtained from wild-type *E. coli* MG1655 (left) and the Pgi mutant (right). A: Phenylalanine C^{α}; B: alanine C^{α}; C: aspartate C^{α}; D: glutamate C^{α}; E: histidine C^{β}; and F: histidine C^{δ}. The carbon atoms are derived from the metabolic intermediates given in the panels. In each panel, the relative abundances of the different carbon fragments shown in (A) are indicated, where carbon–carbon bonds that remained intact during amino acid biosynthesis from glucose are shown in bold. E: The doublet of doublets arising from $^{13}C^{\gamma}$–$^{13}C^{\beta}$–$^{13}C^{\alpha}$ is further split by the two-bond scalar coupling $^{2}J_{C\beta C\delta}$, which reveals the presence of intact C_5-fragments originating from a single source molecule of glucose in ribose, which arise from the action of the oxidative branch of the PP pathway [5,8]. The relative abundancies were calculated as described [3,5] and served to determine the biosynthetic origin of metabolic intermediates (Fig. 3).

hand, exhibited a more balanced TCA cycle use for building block synthesis and energy generation [9].

The METAFoR data of the Pgi mutant differed significantly from those of the wild-type, most pronounced for the flux ratios that are related to the PP pathway (Fig. 3A–D). Most telling is the upper bound of the fraction of PEP molecules that were derived through at least one transketolase reaction (Fig. 3B), which is at around 5–10% for the wild-type but almost 100% for the mutant. This strongly suggests that glucose catabolism proceeds predominantly via the PP pathway in the mutant. Consistently, the fraction of P5P molecules that were not affected by fast exchange via transketolase is increased in the mutant (Fig. 3A). Furthermore, the fraction of OAA originating from PEP (Fig. 3E) was reduced more than twofold in the mutant, when compared to the wild-type. This shows that the TCA cycle operates predominantly for the generation of ATP in the mutant.

Consistent with previous results [12], the primary flux response to Pgi inactivation appears to be the flux rerouting via the PP pathway. METAFoR analysis by NMR, however, provides an upper bound for the fraction of PEP molecules that were derived via transketolase, and we thus cannot exclude residual glucose catabolism via the ED pathway based on the labeling data [5]. In fact, ED pathway in vitro activity (conversion of 6PG to PYR) was identically low in glucose-grown cultures of both strains (1.2 ± 0.1 U mg^{-1} protein). Hence, we conclude that the ED pathway likely catalyzes a minor fraction of glucose catabolism in both wild-type and mutant strain. Consequently, the physiological consequences of PP pathway flux rerouting due to a Pgi knock-out is apparently manifested in significantly reduced specific growth and glucose-uptake rates, and thus a kinetic limitation of glucose catabolism.

3.3. *UdhA overexpression increases μ_{max} of the Pgi mutant*

Kinetic limitations of catabolism might be due to (i) the difficulty of *E. coli* metabolism to reoxidize NADPH, (ii) the inability of the PP pathway to support higher fluxes, or (iii) the inhibition of one or more essential reactions by accumulation of metabolites. Since we have no evidence for the latter possibility (iii) from HPLC analysis of culture supernatants, the first two possibilities appear more likely. Reoxidation of NADPH can potentially be achieved by three reactions in *E. coli*: (i) the NADPH-dependent malic enzyme (either via backflux through the NADH-dependent malic enzyme or via a futile cycle from PYR via MAL, OAA, and PEP to PYR); (ii) the membrane-bound transhydrogenase PntAB [18]; and (iii) the soluble transhydrogenase UdhA [17] (Fig. 1). Significant involvement of the malic enzyme can be excluded because virtually no PYR originates from MAL (Fig. 3G), and only a small fraction of PEP originates from OAA (Fig. 3F). Similarly, PntAB is unlikely to catalyze sufficient reoxidation of NADPH because *pgi*$^{-}$ *pntAB*$^{-}$ double mutants grow as slowly as the *pgi*$^{-}$ mutant [19], i.e. the additional knock-out of PntAB does not further reduce the rate of glucose catabolism, which would be expected if reoxidation through PntAB would play an important role. The primary metabolic function of PntAB appears to be in the generation of NADPH because *zwf*$^{-}$ *pnt*$^{-}$

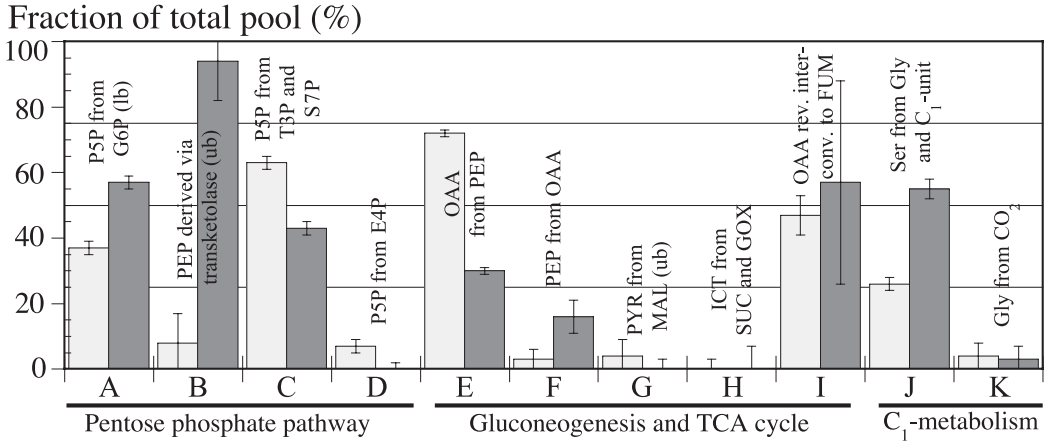

Fig. 3. Origins of metabolic intermediates (A–K) during aerobic exponential growth of *E. coli* MG1655 (white bars) and the Pgi mutant (gray bars). In certain cases, the NMR data permit the determination only of upper bounds (ub) or lower bounds (lb) on the origin of metabolites. The experimental error was estimated from the analysis of redundant ^{13}C scalar coupling fine structures and the signal-to-noise ratio of the [^{13}C–^{1}H]COSY spectra employing the Gaussian law of error propagation. The fraction of the total pool for a particular metabolite quantifies the ratio of this metabolite that is derived from a specified substrate to the sum of all other substrates that contribute to the pool of this metabolite. In cases where only two reactions contribute to one metabolite, e.g. OAA from PEP and PEP from OAA, the remaining fraction of the total pool can be attributed to the competing reaction. Abbreviations are explained in Fig. 1.

mutants grow slower than a *zwf*$^{-}$ mutant [19], as is expected when PntAB produces NADPH in the absence of PP-pathway fluxes (in the *zwf* mutant).

To verify that insufficient reoxidation of NADPH is relevant for the kinetic limitation of glucose catabolism in Pgi mutants, we thus overexpressed the soluble transhydrogenase UdhA in both wild-type and Pgi mutant. The IPTG-induced expression level was chosen such that two- to three-fold increased transhydrogenase activity was achieved, when compared to controls of the same strain that were transformed with the empty p*Trc99*a and subjected to the same IPTG concentration. While this moderate overexpression had no effect on μ_{max} of the wild-type, μ_{max} of the Pgi mutant was increased by about 25% (from 0.22 ± 0.00 to 0.27 ± 0.01 h^{-1}). This observation provides the first evidence for a physiological role of the soluble transhydrogenase UdhA in the reoxidation of NADPH. A further increase in UdhA overexpression to a transhydrogenase activity about 10-fold the control activity did not lead to a further increase in μ_{max} (data not shown). Thus, growth of the Pgi mutant cannot be restored fully to wild-type rates by further improving the capacity for NADPH reoxidation. This suggests that reduced growth of the Pgi mutant is caused by both the increased demand for NADPH reoxidation and the limited capacity of the PP pathway.

Acknowledgements

We are grateful to G. Sprenger for sharing the Pgi mutant with us. T.S. is indebted to the University at Buffalo, The State University of New York, for a start-up fund.

References

[1] Fraenkel, D.G. and Vinopal, R.T. (1973) Carbohydrate metabolism in bacteria. Annu. Rev. Microbiol. 27, 69–100.
[2] Wiechert, W. (2001) ^{13}C metabolic flux analysis. Metab. Eng. 3, 195–206.
[3] Szyperski, T. (1998) ^{13}C-NMR, MS and metabolic flux balancing in biotechnological research. Q. Rev. Biophys. 31, 41–106.
[4] Sauer, U., Szyperski, T. and Bailey, J.E. (2000) Future trends in complex microbial reaction studies. In: NMR in Microbiology: Theory and Applications (Barbotin, J.-N. and Portais, J.-C., Eds.), pp. 479–490. Horizon Scientific Press, Wymondham.
[5] Szyperski, T. (1995) Biosynthetically directed fractional ^{13}C-labeling of proteinogenic amino acids: an efficient analytical tool to investigate intermediary metabolism. Eur. J. Biochem. 232, 433–448.
[6] Szyperski, T., Glaser, R.W., Hochuli, M., Fiaux, J., Sauer, U., Bailey, J.E. and Wüthrich, K. (1999) Bioreaction network topology and metabolic flux ratio analysis by biosynthetic fractional ^{13}C-labeling and two-dimensional NMR spectroscopy. Metab. Eng. 1, 189–197.
[7] Maaheimo, H., Fiaux, J., Çakar, Z.P., Bailey, J.E., Sauer, U. and Szyperski, T. (2001) Central carbon metabolism of *Saccharomyces cerevisiae* explored by biosynthetic fractional ^{13}C labeling of common amino acids. Eur. J. Biochem. 268, 2464–2479.
[8] Sauer, U., Hatzimanikatis, V., Bailey, J.E., Hochuli, M., Szyperski, T. and Wüthrich, K. (1997) Metabolic fluxes in riboflavin-producing *Bacillus subtilis*. Nat. Biotechnol. 15, 448–452.
[9] Sauer, U., Lasko, D.R., Fiaux, J.M.H., Glaser, R., Szyperski, T., Wüthrich, K. and Bailey, J.E. (1999) Metabolic flux ratio analysis of genetic and environmental modulations of *Escherichia coli* central carbon metabolism. J. Bacteriol. 181, 6679–6688.
[10] Gottschalk, G. (1986) Bacterial Metabolism. Springer-Verlag, New York.
[11] Böhringer, J., Fischer, D., Mosler, G. and Hengge-Aronis, R. (1995) UDP-glucose is a potential intracellular signal molecule in the control of expression of σ^{s} and σ^{s}-dependent genes in *Escherichia coli*. J. Bacteriol. 177, 413–422.
[12] Fraenkel, D.G. and Levisohn, S.R. (1967) Glucose and gluconate metabolism in an *Escherichia coli* mutant lacking phosphoglocose isomerase. J. Bacteriol. 93, 1571–1578.

[13] Park, S.M., Sinskey, A.J. and Stephanopoulos, G. (1997) Metabolic and physiological studies of *Corynebacterium glutamicum*. Biotechnol. Bioeng. 55, 864–879.
[14] Dauner, M. and Sauer, U. (2001) Stoichiometric growth model for riboflavin-producing *Bacillus subtilis*. Biotechnol. Bioeng. 76, 132–143.
[15] Allenza, P. and Lessie, T.G. (1982) *Pseudomonas cepacia* mutants blocked in the Entner Doudoroff pathway. J. Bacteriol. 150, 1340–1347.
[16] Glaser, R. (1999) FCAL 2.3.0.
[17] Boonstra, B., French, C.E., Wainwright, I. and Bruce, N.C. (1999) The *udhA* gene of *Escherichia coli* encodes a soluble pyridine nucleotide transhydrogenase. J. Bacteriol. 181, 1030–1034.
[18] Clarke, D.M., Loo, T.W., Gillam, S. and Bragg, P.D. (1986) Nucleotide sequence of the *pntA* and *pntB* genes encoding the pyridine nucleotide transhydrogenase of *Escherichia coli*. Eur. J. Biochem. 158, 647–653.
[19] Hanson, R.L. and Rose, C. (1980) Effects of insertion mutation in a locus affecting pyridine nucleotide transhydrogenase (*pnt*::Tn5) on the growth of *Escherichia coli*. J. Bacteriol. 141, 401–404.